



## Adsorptive removal of bisphenol A from aqueous solution using metal-organic frameworks

Feng-Xiang Qin<sup>a</sup>, Shao-Yi Jia<sup>a</sup>, Yong Liu<sup>b</sup>, Hao-Yang Li<sup>a</sup>, Song-Hai Wu<sup>a,\*</sup>

<sup>a</sup>School of Chemical Engineering and Technology, Tianjin University, Tianjin, P.R. China

Tel. +86 022 87401961; Fax: +86 022 87401961; email: [songhaiwu@gmail.com](mailto:songhaiwu@gmail.com)

<sup>b</sup>School of Chemistry & Chemical Engineering, Tianjin University of Technology, Tianjin, P.R. China

Received 8 July 2013; Accepted 9 December 2013

### ABSTRACT

Adsorptive removal of bisphenol A (BPA) from aqueous solution has been studied over two highly porous metal-organic frameworks (MIL-101(Cr) and MIL-100(Fe)) in view of the adsorption kinetics, adsorption isotherm, effect of initial pH and effect of ionic strength. The adsorption kinetics fit pseudo-second-order kinetic model well and the adsorption isotherms follow the Langmuir model. The adsorption kinetics and capacity of BPA over MIL-101(Cr) generally depend on the average pore size and specific surface area (or pore volume), respectively. The adsorption mechanism may be explained with  $\pi$ - $\pi$  interaction and hydrogen bonding between BPA and MIL-101(Cr). Finally, it can be suggested that metal-organic frameworks possessing high porosity and large pore size can be used as potential adsorbents to remove harmful endocrine disrupting chemicals in contaminated water.

*Keywords:* Endocrine disrupting chemicals (EDCs); Metal-organic framework (MOF); Bisphenol A(BPA); Adsorption; Kinetics

### 1. Introduction

Recently, the environmental pollution of phenolic endocrine disrupting chemicals (EDCs), which may cause negative effects on the endocrine systems of humans and wildlife, have aroused public concerns as these contaminants were frequently detected in different water sources and factory effluents [1,2]. Bisphenol A (BPA) [2,2-bis(4-hydroxyphenyl)propane, Fig. 1], as one of the phenolic EDCs, has been widely used in industries as raw materials for epoxy and polycarbonate plastics, such as baby bottles, lining of food cans and dental sealants [3]. Due to the worldwide annual growing demand of household and

commercial products, large amount of BPA have been released into the aquatic environment and they have been observed in landfill leachates, rivers, seas and soils. Besides, toxicity studies have found that BPA is one of the EDCs [4], which may cause various adverse effects on aquatic organisms even at low exposure levels [5,6]. Accordingly, there is an urgent need for developing an effective technology to remove BPA from aquatic environment.

Conventional physical and chemical treatment technologies for the removal of BPA include adsorption, ozonation and advanced oxidation processes [7,8]. Among them, physical adsorption is generally considered as an effective and fast removal method. Activated carbon (AC) which has been widely used in

\*Corresponding author.

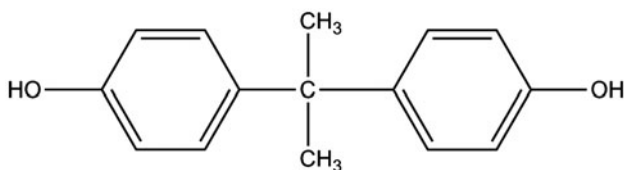


Fig. 1. Molecular structure of BPA used as adsorbate in the study.

the removal of organic molecules has also been studied for the removal of BPA from aqueous solution [9]. Commercial carbons (W20 and F20) selectively modified with nitric acid and thermal treatment under  $N_2$  have been used to adsorb BPA from aqueous solution [10]. W20 and its thermally modified sample (W20 N) have better equilibrium adsorption amounts as high as 382.12 and 432.34 mg/g. Moreover, other adsorbents such as minerals and carbon adsorbents [11], carbon nanomaterials [12], single-walled carbon nanotubes [13], sewage sludge [14], natural biosorbent and modified peat [15], soil column [16], and highly ordered mesoporous carbon CMK-3 [17] have also been studied for the removal of BPA.

Metal-organic frameworks (MOFs), which exhibit high surface area and large pore volume, have attracted considerable attention due to their elegant topology and diverse applications in catalysis [18,19], separations [20,21], drug delivery [22–24], gas storage [25,26] and sensing [27,28]. Recently, more and more investigations about MOF materials are concentrating on the removal of harmful materials such as S-compounds [29,30], dyes [31–33], N-containing compounds [34], benzene [35],  $Hg^{2+}$  [36], phenol [37], pharmaceuticals and personal-care products (PPCPs) [38], C60 and C70 [39] from fuel, wastewater or gases due to their unique characteristics [40,41].

Among the numerous MOFs reported so far, two of the most classical materials are the porous chromium-benzenedicarboxylate (Cr-BDC called as MIL-101(Cr), MIL stands for Material of Institute Lavoisier) [42] and iron-benzenetricarboxylate (Fe-BTC named MIL-100(Fe)) [43] which are largely studied for their potential applications because of their high pore volume, larger pore size, and high thermal and chemical stability. MIL-101(Cr) with a chemical formula of  $Cr_3O(F/OH)(H_2O)_2[C_6H_4(CO_2)_2]$  possesses several unprecedented features such as a mesoporous zeotype architecture with mesoporous cages (29 and 34 Å) and microporous windows (12 and 16 Å in diameter), huge pore volume (1.9  $cm^3/g$ ), fantastic high specific surface area (as high as  $4,100 \pm 200 m^2/g$ ), and numerous unsaturated chromium sites (up to theoretically

approximately 3.0 mmol/g) [44]. MIL-101(Cr) has been investigated for adsorptive removal of dyes [31,32], benzene [35] and PPCPs [38] from aqueous solution. MIL-100(Fe) with a chemical formula  $Fe_3^{(III)}OF(H_2O)_2[C_6H_3(CO_2)_3]_2 \cdot nH_2O$  ( $n \sim 14.5$ ) has two types of large accessible and permanent pores (25 and 29 Å in diameter) with microporous windows (5.5 and 8.6 Å in diameter) [43]. MIL-100(Fe) has been studied for the adsorption of malachite green from aqueous solution by Huo and Yan [45]. It has also been used for selective removal of N-heterocyclic aromatic contaminants from fuels [34].

However, to our all knowledge, there are only two research papers about the use of MOFs in the removal of EDCs so far [46,47]. In this work, we have investigated the adsorption of one of the typical EDCs (BPA) over MIL-101(Cr), MIL-100(Fe) and AC performing as a control material for the first time, especially well studied of MIL-101(Cr), MIL-100(Fe), to understand the characteristics of adsorption and possibility of using MOFs as adsorbents for the removal of EDCs, hazardous materials, from wastewater.

## 2. Experimental

### 2.1. Materials and reagents

All solvents and reactants were commercially available and were used without further purification. Terephthalic acid (TPA, 98%) and 1,3,5-benzenetricarboxylic acid ( $H_3BTC$ , 95%) were obtained from Aldrich. AC, BPA (99%), chromium nitrate nonhydrate ( $Cr(NO_3)_3 \cdot 9H_2O$ , 99%), iron powder (97%), hydrofluoric acid (HF, 48%), nitric acid ( $HNO_3$ , 60%) and N,N'-dimethylformamide (DMF, 99%) were purchased from Tianjin Guangfu Fine Chemical Research Institute, China.

MIL-101(Cr) was synthesized by  $Cr(NO_3)_3 \cdot 9H_2O$ , TPA and deionized water according to a reported method [48]. Typically, a mixture of  $Cr(NO_3)_3 \cdot 9H_2O$  1.2 g, terephthalic acid 500 mg and HF 0.6 mL (5 M) in  $H_2O$  (15 mL) was heated in a Teflon-lined stainless steel autoclave at 220°C for 8 h. The resulting green-coloured products in the solution were passed through a coarse glass filter (G1, 20–30  $\mu m$ ) to remove the unreacted colourless crystals of free terephthalic acid. Then, the as-synthesized MIL-101(Cr) was further purified by treatments with hot DMF (100°C, 8 h, 2 times), 1 M of  $NH_4F$  (70°C, 24 h) and hot EtOH (80°C, 8 h, 2 times), filtered off (G4, 3–4  $\mu m$ ), and dried overnight in an oven at 150°C under air atmosphere.

MIL-100(Fe) was synthesized according to Horcajada et al. [49]. Typically, iron powder 277.5 mg,

H<sub>3</sub>BTC 687.5 mg, hydrofluoric acid 200  $\mu$ L and nitric acid 190  $\mu$ L were well mixed with deionized water 20 mL in a Teflon-lined steel autoclave. The autoclave was then placed in an oven at 150°C for 12 h. After cooling to room temperature, the light-orange solid products were collected by filtration, and then they were washed with deionized water. The as-synthesized MIL-100(Fe) was further purified with boiling water and hot ethanol. Then the highly purified MIL-100(Fe) was collected by centrifugation at 10,000 rpm for 10 min. The solid was finally dried at 80°C under vacuum overnight.

## 2.2. Characterization of the materials

The synthetic MOFs were characterized by X-ray diffraction (XRD) and BET-N<sub>2</sub> sorption method. XRD patterns in the  $2\theta$  range of 2–20° were collected at ambient temperature using Cu-K $\alpha$  radiation on Rigaku D/max 2200/PC diffractometer (Rigaku Corporation, Japan). Nitrogen adsorption and desorption isotherms were measured at 77 K using a Tristar3000 volumetric adsorption analyser (Micromeritics Instrument Corporation, USA) after the samples were first outgassed at 90°C for 1 h and then degassed at 180°C for 3 h in nitrogen atmosphere. Specific surface areas were determined by the BET method and the mesopore size distribution was determined by the Barrett-Joyner-Halenda (BJH) method.

## 2.3. Adsorption experiments

BPA solution of different concentrations was prepared using deionized water. The BPA concentrations were determined via measuring the absorbance of the solutions at 275 nm with a spectrophotometer (Phenix UV spectrophotometer, UV-1700). The calibration curve was obtained from the spectra of the standard solutions (20–100 ppm) at natural pH (pH 5.6).

Before adsorption, all the adsorbents were kept in a desiccator and dried overnight under vacuum at 100°C. For the kinetic studies, an exact amount of the adsorbents (20.0 mg) were put into 100 mL of fixed BPA concentrations from 20 to 300 ppm. The adsorption was carried out at 30°C and the flask containing both adsorbents and BPA was kept in a thermostatic bath with constant agitation (170 rpm). After adsorption for a pre-determined time, the concentrations of BPA in solution were analysed with different time intervals (0, 5, 15, 30, 60, 120 and 180 min) after the solids were separated by centrifugation (12,000 rpm for 5 min). The BPA concentration was calculated according to the absorbance of the UV spectra. Control

experiments were performed with 100 mL deionized water instead of BPA solution. The amount of BPA adsorbed onto different adsorbents was calculated by mass balance relationship Eq. (1):

$$q_t = (C_0 - C_t) \frac{V}{W} \quad (1)$$

where  $C_0$  and  $C_t$  (mg/L) are the liquid-phase concentrations of the BPA at time = 0 and  $t$ , respectively.  $V$  (L) and  $W$  (g) are the volume of the solution and the weight (g) of the adsorbents, respectively.

To determine the adsorption capacity at various conditions of acidity, the initial pH values (pH 3.0–11.0) of the BPA solution was adjusted with 0.1 M HCl or 0.1 M NaOH aqueous solution. The adsorption kinetics of BPA under different ionic strengths (I) ranging from 5 to 500 mM by adding NaCl solution was also conducted.

## 3. Results and discussion

### 3.1. Characterization and properties of adsorbents

As shown in Fig. 2(a), XRD analysis showed that the as-prepared MIL-101(Cr) and MIL-100(Fe) materials are crystallines and in good agreement with the simulated results [48,49]. The BET surface areas and pore volumes of the materials measured by N<sub>2</sub> adsorption at 77 K are shown in Table 1. The values are in good agreement with most of those reported in previous papers [48,49]. The BET of the three adsorbents are in the order of MIL-100(Fe) < AC < MIL-101(Cr). The pore size distribution of MIL-101(Cr) estimated using the BJH method gives a pore diameter of maxima at 25.2 Å. However, there is no apparent mesoporous in MIL-100(Fe) from the pore size distribution pattern (see Fig. 2(b)).

### 3.2. Adsorption kinetics

The effects of contact time and BPA concentration (40, 80 and 120 ppm) on the BPA adsorption over different adsorbents are depicted in Fig. 3. As shown in Fig. 3, the adsorbed quantity of BPA is in the order of MIL-100(Fe) < AC < MIL-101(Cr) for the whole adsorption time at any initial BPA concentration. The adsorbed BPA slightly increases with the increase of the initial BPA concentration from 40 to 120 ppm showing the favourable adsorption of BPA at high concentration. The equilibrium adsorption capacity of MIL-101(Cr) is as high as 156.8 mg/g for 120 ppm BPA (see Fig. 3(c)). Moreover, almost all the three adsorbents have got to adsorption equilibrium at 60 min

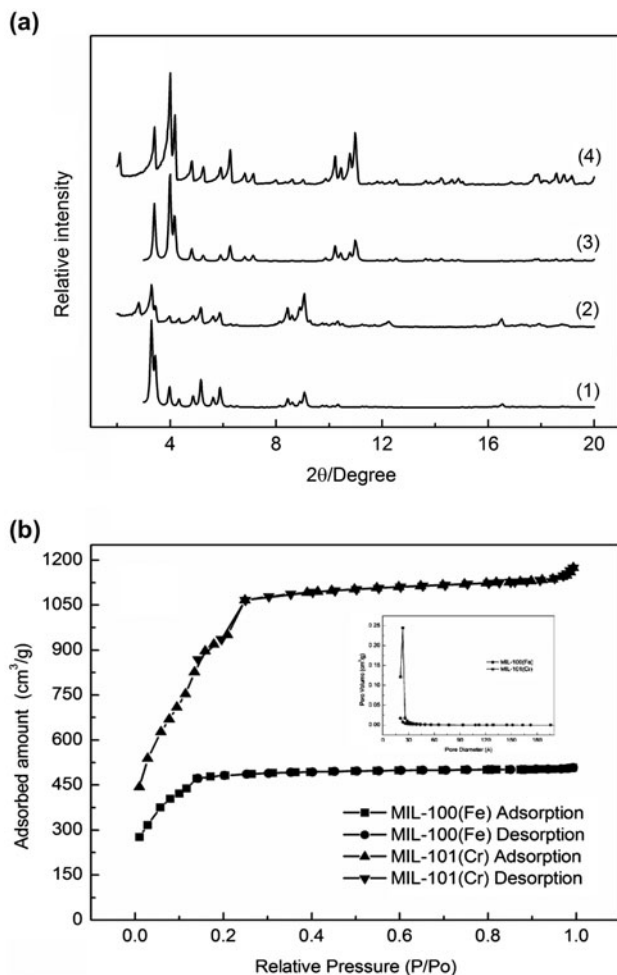


Fig. 2. (a) XRD patterns of MIL-101(Cr) and MIL-100(Fe). Simulated patterns from the crystallographic data of (1) MIL-101(Cr), (3) MIL-100(Fe); XRD patterns of (2) MIL-101(Cr), (4) MIL-100(Fe) synthesized using hydrothermal synthesis. (b) N<sub>2</sub> adsorption-desorption isotherms of as-synthesized MOFs and the pore size distribution of the materials (inset).

except AC, showing the rapid adsorption of BPA over MIL-100(Fe) and MIL-101(Cr).

Table 1  
The textural properties of the three adsorbents

Adsorbent	$S_{\text{BET}}^{\text{a}}$ (m <sup>2</sup> /g)	$S_{\text{Langmuir}}^{\text{b}}$ (m <sup>2</sup> /g)	Total pore volume (cm <sup>3</sup> /g)	Mean pore diameter <sup>c</sup> (Å)
MIL-101(Cr)	3,711	5,462	1.77	25.2
MIL-100(Fe)	1,754	2,420	0.78	27.5
AC	2,535	n.d.	1.65	5.7

<sup>a</sup> $S_{\text{BET}}$  is the BET specific surface area.

<sup>b</sup> $S_{\text{Langmuir}}$  is Langmuir surface area.

<sup>c</sup>Mean pore diameter is BJH desorption average pore diameter calculated by  $4V/A$ .

n.d. means not detected.

To compare the adsorption kinetics precisely, the changes of adsorption amount with time are treated with the versatile pseudo-second-order kinetic model [50,51] which is expressed by the following equations:

$$q_t = \frac{q_e^2 k_2 t}{1 + q_e k_2 t} \quad (2)$$

$$\text{or, } \frac{t}{q_t} = \frac{1}{q_e^2 k_2} + \frac{1}{q_e} t \quad (3)$$

where  $q_e$  (mg/g) is amount adsorbed at equilibrium;  $q_t$  (mg/g) is amount adsorbed at time  $t$ ;  $t$  (min) is adsorption time;  $k_2$  (g/(mg min)) is the pseudo-second-order rate constant.

Therefore, the second-order-kinetic constant ( $k_2$ ) can be calculated by  $k_2 = \text{slope}^2 / \text{intercept}$  when the  $t/q_t$  is plotted against  $t$ .

The calculated kinetic constants ( $k_2$ ) and correlation coefficients ( $R^2$ ) are shown in Table 2. According to the correlation coefficient ( $R^2$ ), the relative high  $R^2$  values show that the BPA adsorption over the three adsorbents at three different initial concentrations fits the pseudo-second-order kinetics model well. Additionally, from Table 2, the  $q_{e,\text{cal}}$  value calculated with this model is in good agreement with experimental data  $q_{e,\text{exp}}$ . The adsorption kinetic constants for BPA adsorption list in the order of  $\text{AC} < \text{MIL-100(Fe)} < \text{MIL-101(Cr)}$ . The adsorption kinetic constants for BPA adsorption over MIL-101(Cr) and over MIL-100(Fe) are larger than the constants over AC. The reason may be that the pore diameters of MIL-101(Cr) and MIL-100(Fe) are larger than that of AC which is a microporous material. The kinetic constants of the three adsorbents increase slightly as the initial BPA concentrations increase, exhibiting rapid adsorption in the presence of BPA in high concentration, similar to previous reports [52,53]. Moreover, as shown in Table 2, for all three adsorbents, amount adsorbed at equilibrium ( $q_e$ ) also perform the

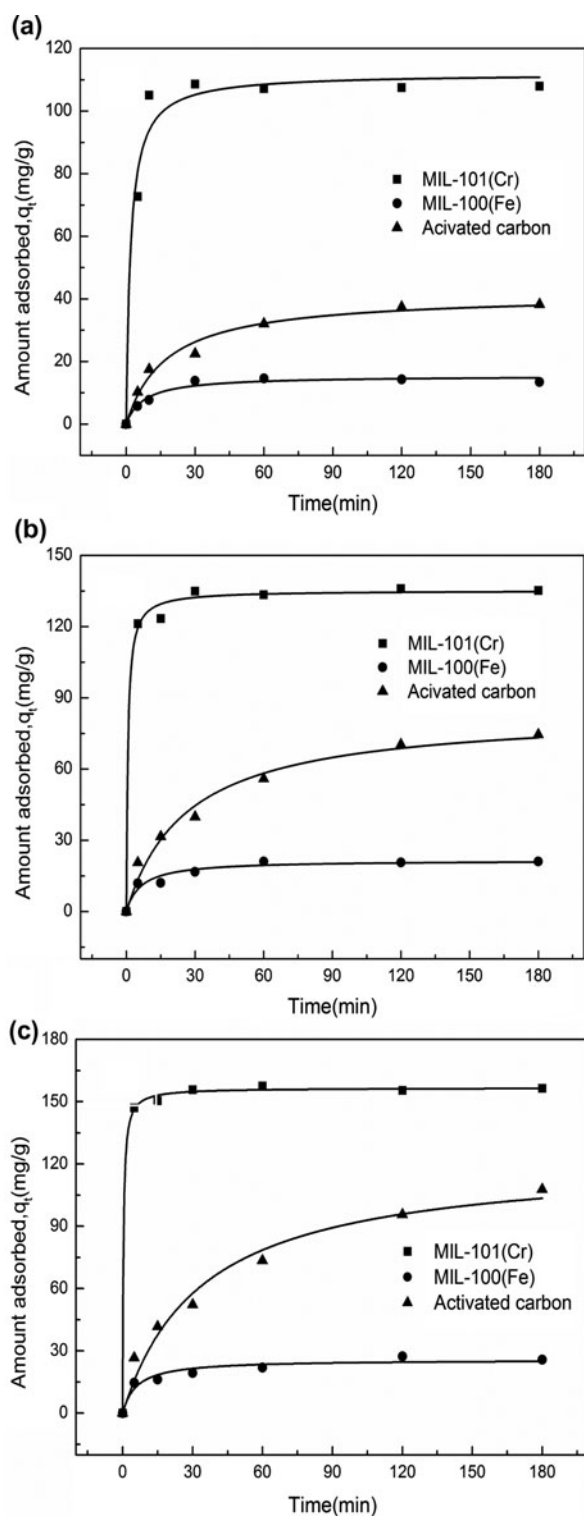


Fig. 3. Effects of contact time and initial BPA concentration on the adsorption of BPA over the three adsorbents: (a)  $C_i = 40$  ppm; (b)  $C_i = 80$  ppm; and (c)  $C_i = 120$  ppm.

same tendency. This may be attributed to the fact that higher initial concentration provides a higher driving

force to overcome all mass transfer resistances of solutes between the aqueous and solid phases [54]. The equilibrium adsorption capacity ( $q_{e,cal}$ ) over MIL-101(Cr) which is as high as 156.8 mg/g at 120 ppm is much larger than those over the other two adsorbents. Therefore, MIL-101(Cr) is the most effective adsorbent for BPA removal in the viewpoint of adsorption amount and rate.

The fast adsorption of BPA over MIL-101(Cr), compared to the adsorption over MIL-100(Fe), is probably due to the larger pore size (see Fig. 2(b)) of MIL-101(Cr) as the kinetic constant of adsorption generally increases with the increasing pore size of a porous material in liquid-phase adsorption [35]. Moreover, the larger adsorption capacity of MIL-101(Cr) is due to the larger BET of MIL-101(Cr) than AC and MIL-100(Fe) (see Table 1). Compared to MIL-100(Fe), the larger kinetics constants of MIL-101(Cr) are caused by the mesoporous pore structure in MIL-101(Cr). It should be noted that the size of the BPA molecule is calculated to be  $0.94 \times 0.59 \times 0.48$  nm [55]. The large apertures of the MIL-101(Cr) (12.6 Å) allow easy introduction of BPA, whereas the small dimensions of the pentagonal windows of MIL-100(Fe) (8.6 Å, close to the BPA size) are limited for a valuable introduction of the guest in MIL-100(Fe).

### 3.3. Adsorption isotherms

Adsorption experiments of MIL-101(Cr), MIL-100(Fe) and AC at different initial BPA concentrations from 40 to 300 ppm have been carried out to get adsorption kinetics parameters. The adsorption isotherms were obtained after adsorption for sufficient time of 2 h, and the results are shown in Fig. 4(a). The amount of adsorbed BPA over MIL-101(Cr) is much higher than that of MIL-100(Fe) and AC under similar experimental conditions, suggesting the efficiency of the mesoporous MIL-101(Cr) in the adsorption of BPA. In this study, Langmuir model [54] assuming monolayer adsorption onto a surface which consists of finite number of active sites with a uniform energy has been used to describe the adsorption isotherms. The linear form of Langmuir isotherm equation [51,56] is given as:

$$\frac{C_e}{q_e} = \frac{C_e}{Q_0} + \frac{1}{Q_0 b} \quad (4)$$

where  $C_e$  is the equilibrium concentration of adsorbate (mg/L);  $q_e$  is the amount of adsorbate adsorbed (mg/g);  $Q_0$  is the Langmuir constant (maximum

Table 2

The pseudo-second-order kinetic constants ( $k_2$ ) with correlation coefficients ( $R^2$ ) for the adsorption of BPA over three adsorbents at various initial concentrations obtained from non-linear regression method

Adsorbents	Pseudo-second-order kinetics constants $k_2$ (g/(mg min))											
	120 ppm				80 ppm				40 ppm			
	$q_{e,exp}$ (mg/g)	$q_{e,cal}$ (mg/g)	$k_2$	$R^2$	$q_{e,exp}$ (mg/g)	$q_{e,cal}$ (mg/g)	$k_2$	$R^2$	$q_{e,exp}$ (mg/g)	$q_{e,cal}$ (mg/g)	$k_2$	$R^2$
MIL-101(Cr)	156.4	156.8	$1.39 \times 10^{-2}$	1.0	135.9	135.2	$8.75 \times 10^{-3}$	1.0	107.9	112.0	$3.84 \times 10^{-3}$	0.995
MIL-100(Fe)	26.0	25.9	$3.77 \times 10^{-3}$	0.997	21.0	21.6	$2.81 \times 10^{-3}$	0.996	14.3	15.5	$2.26 \times 10^{-3}$	0.981
AC	134.2	113.5	$0.84 \times 10^{-3}$	0.998	75.7	88.6	$0.34 \times 10^{-3}$	0.998	38.3	44.8	$0.17 \times 10^{-3}$	0.992

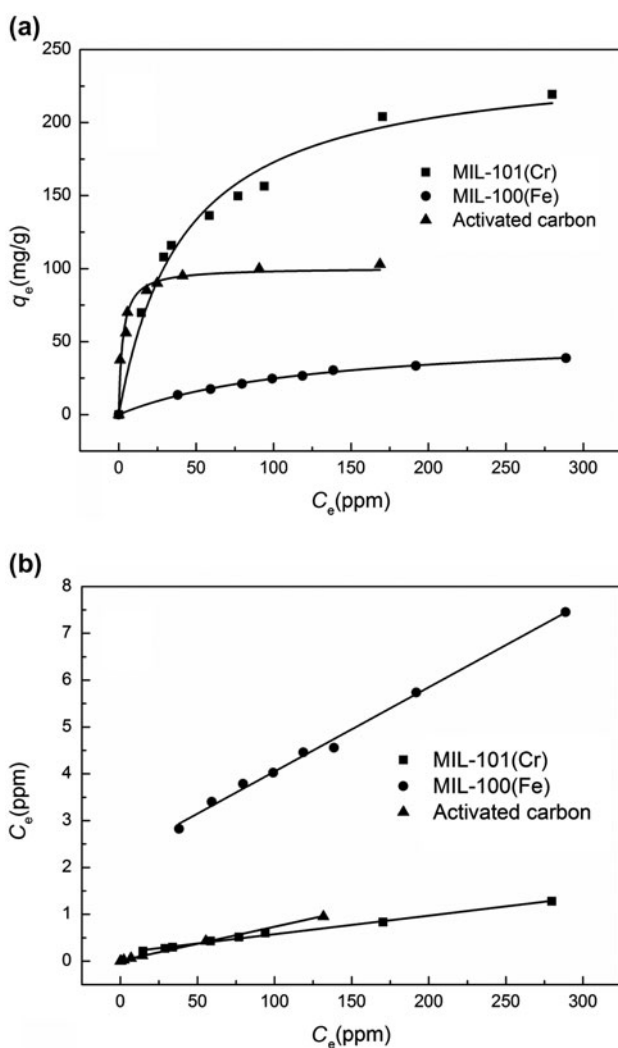


Fig. 4. (a) Adsorption isotherms for BPA adsorption over MIL-101, MIL-100-Fe and AC. (b) Langmuir plots of the isotherms of (a).

adsorption capacity) (mg/g); and  $b$  is the Langmuir constant (L/mg or L/mol).

So, the  $Q_0$  can be obtained from the reciprocal of the slope of a plot of  $C_e/q_e$  against  $C_e$ . Fig. 4(b) shows the linear Langmuir plots for the adsorption of BPA over the three adsorbents, and the  $Q_0$  values determined from Fig. 4(b) are summarized in Table 3.

As shown in Table 3, the data of the adsorption of BPA under the experimental conditions fit quite well with linear regression curve (correlation coefficient,  $R^2 > 0.990$ ). These results indicated that the adsorption of BPA onto the three adsorbents was a typical monomolecular-layer adsorption. Generally, the maximum monolayer capacity  $Q_0$  increases in the order of MIL-100(Fe) < AC < MIL-101(Cr) and the maximum adsorption capacity over MIL-101(Cr) is 252.5 mg/g, which is 4.54 times and 1.84 times higher than that of MIL-100(Fe) and AC, respectively, confirming the great potential application of MIL-101(Cr) in the adsorptive removal. Many researchers have reported that adsorbents having larger pore volume or BET can adsorb more solute which results in larger  $Q_0$  value [57]. In our study, we have also found that the  $Q_0$  values of BPA adsorption increase with increase of BET or pore volume (see Table 1).

### 3.4. Effect of initial pH

The adsorption of BPA has been usually affected by the pH [9]. BPA adsorption at various pH values was measured after equilibration with MIL-101(Cr)

Table 3

Langmuir isotherm parameters for the BPA adsorption over MIL-101(Cr), MIL-100(Fe) and AC

Adsorbents	Langmuir parameters		
	$b$ (L/mg)	$Q_0$ (mg/g)	$R^2$
MIL-101(Cr)	$2.22 \times 10^{-2}$	252.5	0.993
MIL-100(Fe)	$8.01 \times 10^{-3}$	55.6	0.995
AC	0.995	137.0	0.999

and MIL-100(Fe). BPA adsorption over MIL-101(Cr) and MIL-100(Fe) was studied for a fixed BPA concentration of 80 ppm and a fixed time of 2 h at various initial pH. As shown in Fig. 5, pH had an evident effect on BPA sorption capacity. The adsorption equilibrium amounts of BPA over MIL-101(Cr) at pH 3.0 and 5.6 were 139.9 and 136.3 mg/g, respectively. MIL-101(Cr) represented the highest adsorption equilibrium capacity (152.9 mg/g) at pH 7.0. It is reported that the pKa value of BPA ranges from 9.6 to 10.2 [58], implying that BPA is electropositive at  $\text{pH} < 9.0$  and is electronegative at  $\text{pH} > 10.0$ . It is reported that the zeta potential of MIL-101(Cr) is positive below pH 9.0 and it is more positive when pH ranges from 3.0 to 6.0 than that of 7.0 [33]. Therefore, the less  $q_e$  over MIL-101(Cr) at pH 3.0 ( $q_e$ , 139.9 mg/g) and pH 5.6 ( $q_e$ , 136.3 mg/g) than that of pH 7.0 ( $q_e$ , 152.9 mg/g) might be due to the fact that the sorbents in acidic medium was occupied by  $\text{H}^+$ , and the  $\pi$ - $\pi$  interaction gave adsorption affinity for BPA. At a neutral pH, hydrogen bonding between BPA and MIL-101(Cr) and  $\pi$ - $\pi$  interaction were responsible for the sorption of BPA. Moreover, the great reduction in the adsorption equilibrium capacity from 143.2 mg/g (pH 9.0) to 114.4 mg/g (pH 11.0) of MIL-101(Cr) may be consequent on that BPA was mostly ionized to mono- or divalent anions ( $\text{BPA}^-$  and  $\text{BPA}^{2-}$ ) in basic solution and the hydrogen bonding between BPA and sorbents disappeared [59]. However, the  $q_e$  of MIL-100(Fe) changes little from pH 3.0 to 9.0. The largest  $q_e$  is 32.0 mg/g at pH 7.0. According to the literature, negative charges exist on the surface of MIL-100(Fe) as the pH change from 2.0 to 10.0 [33]. When the solution pH was similar to the pKa value

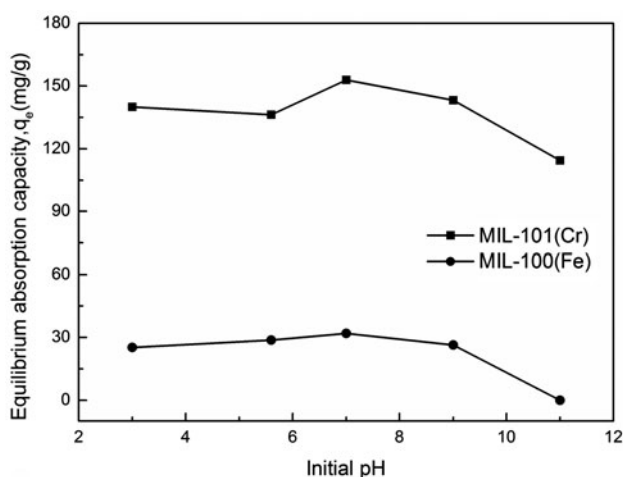


Fig. 5. Effect of pH on the adsorbed amount of BPA over MIL-101(Cr) and MIL-100(Fe), other conditions:  $C_i$ , 80 ppm; adsorption time, 2 h; temperature, 30°C and adsorbent concentration, 200 ppm.

(pH 9.0) of BPA, the ionization degree of BPA was near to zero, thus weakening the electrostatic attraction interaction. The repulsive electrostatic interaction was dominating at  $\text{pH} > 10.0$ . Moreover, the adsorption capacity for MIL-100(Fe) at pH 11 was 0, which might result from the dissolution of MIL-100(Fe) at pH 11.

### 3.5. Effect of ionic strength

Generally, various salts and metal ions existed in wastewater lead to high ionic strength which may affect the pollutant adsorption onto adsorbents. The adsorption experiments of the effect of the concentration of NaCl on the adsorption of BPA over MIL-101(Cr) and MIL-100(Fe) have been carried out with three different ionic strengths. The results are shown in Fig. 6. From Fig. 6(a), we can see that equilibrium

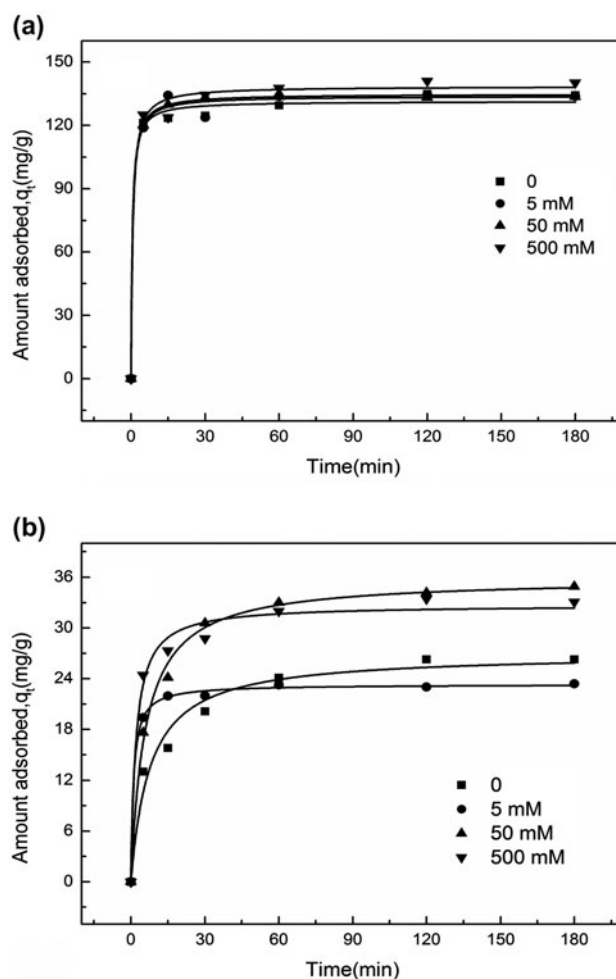


Fig. 6. Effect of concentration of NaCl on the adsorption of BPA over MIL-101(Cr) and MIL-100(Fe), other conditions:  $C_i$ , 80 ppm; temperature, 30°C; pH natural (pH 5.6) and adsorbent concentration: 200 mg/L.

adsorption amount of MIL-101(Cr) was 131.4 mg/g when there was no NaCl as addition. The equilibrium adsorption amount of MIL-101(Cr) has almost no change when a small amount of NaCl (5 mM or 50 mM) was added into the solution while the  $q_e$  slightly increased to 138.5 mg/g when 500 mM NaCl was added. The results may be due to the fact that the higher concentration of ionic strength could produce a screening effect of the surface charge that favoured the dispersion interaction and consequently enhanced the adsorption of BPA [60]. It is obvious from Fig. 6(b) that there is a decrease in the equilibrium adsorption amount of BPA onto MIL-100(Fe) after 5 mM NaCl was added into the solution. It may be beneficial for the  $\text{Na}^+$  adsorption with electrostatic interaction as the adsorbent is electronegative on the surface at natural pH. Therefore, the existence of  $\text{Na}^+$  on the surface of adsorbent may decrease the adsorption of BPA. However, the adsorbed capacity of MIL-100(Fe) slightly increased with the concentration of NaCl increasing from 50 to 500 mM. However, the increase of ionic strength produced a screening effect of the surface charge and a salting-out effect which enhanced the adsorption of BPA. In addition, the salting-out effect could enhance the BPA adsorption onto MIL-100(Fe). The above results indicate that MIL-101(Cr) adsorbs BPA through  $\pi$ - $\pi$  dispersion interactions between the aromatic ring electrons in the adsorbate and those MOFs to the pore structure while electrostatic interaction is one of the mechanisms for the adsorption of BPA over MIL-100(Fe).

#### 4. Conclusion

The liquid-phase adsorption of BPA onto two MOF materials has been investigated and the experimental data fit well with pseudo-second-order kinetic model. MIL-101(Cr) and MIL-100(Fe) represented better adsorption capacity and the  $q_e$  were 252.5 and 55.6 mg/g. The adsorption capacity and adsorption kinetic constant of MIL-101(Cr) are greater than those of MIL-100(Fe), showing the importance of porosity and pore size for adsorption, which is similar to reported results. Furthermore, the adsorption capacity of BPA onto the two MOFs at various initial pH values indicated that the interaction of the benzene ring on BPA with a hydrophobic benzene ring on the surface of sorbents and the hydrogen bonding of phenolic group on BPA with the surface of sorbents were proposed to sorption affinity between sorbents and BPA. However, the addition of different amount of NaCl proved that BPA was adsorbed into MIL-101(Cr) pore through free diffusion and MIL-100(Fe)

adsorbed BPA with electrostatic interaction. From this study, it can be suggested that the MOF-type materials may be applied in the adsorptive removal of EDC pollutant from contaminated water. Due to the enrichment effect of BPA into the pore structure of MIL-101(Cr), further work has been carried out in our laboratory to investigate efficient catalysts based on MIL-101(Cr) to degrade BPA in contaminated water.

#### Acknowledgements

The author acknowledges the support by the National Natural Science Foundation of China (No. 41003040) and the Natural Science Foundation of Tianjin, P.R. China (No. 10JCYBJJC06000).

#### References

- [1] Z.-H. Liu, Y. Kanjo, S. Mizutani, Removal mechanisms for endocrine disrupting compounds (EDCs) in wastewater treatment – Physical means, biodegradation, and chemical advanced oxidation: A review, *Sci. Total Environ.* 407 (2009) 731–748.
- [2] C. Bicchi, T. Schilirò, C. Pignata, E. Fea, C. Cordero, F. Canale, G. Gilli, Analysis of environmental endocrine disrupting chemicals using the E-screen method and stir bar sorptive extraction in wastewater treatment plant effluents, *Sci. Total Environ.* 407 (2009) 1842–1851.
- [3] C.A. Staples, P.B. Dome, G.M. Klecka, S.T. Oblock, L.R. Harris, A review of the environmental fate, effects, and exposures of bisphenol A, *Chemosphere* 36 (1998) 2149–2173.
- [4] Y.B. Wetherill, B.T. Akingbemi, J. Kanno, J.A. McLachlan, A. Nadal, C. Sonnenschein, C.S. Watson, R.T. Zoeller, S.M. Belcher, In vitro molecular mechanisms of bisphenol A action, *Reprod. Toxicol.* 24 (2007) 178–198.
- [5] M. Muñoz-De-Toro, C.M. Markey, P.R. Wadia, E.H. Luque, B.S. Rubin, C. Sonnenschein, A.M. Soto, Perinatal exposure to bisphenol-A alters peripubertal mammary gland development in mice, *Endocrinology* 146 (2005) 4138–4147.
- [6] T. Suzuki, Y. Nakagawa, I. Takano, K. Yaguchi, K. Yasuda, Environmental fate of bisphenol A and its biological metabolites in river water and their xenoestrogenic activity, *Environ. Sci. Technol.* 38 (2004) 2389–2396.
- [7] M. Deborde, S. Rabouan, J.-P. Duguet, B. Legube, Kinetics of aqueous ozone-induced oxidation of some endocrine disruptors, *Environ. Sci. Technol.* 39 (2005) 6086–6092.
- [8] E.J. Rosenfeldt, K.G. Linden, Degradation of endocrine disrupting chemicals bisphenol A, ethinyl estradiol, and estradiol during UV photolysis and advanced oxidation processes, *Environ. Sci. Technol.* 38 (2004) 5476–5483.
- [9] I. Bautista-Toledo, M.A. Ferro-García, J. Rivera-Utrilla, C. Moreno-Castilla, F.J. Vegas Fernández, Bisphenol A removal from water by activated carbon. Effects of carbon characteristics and solution chemistry, *Environ. Sci. Technol.* 39 (2005) 6246–6250.

- [10] G. Liu, J. Ma, X. Li, Q. Qin, Adsorption of bisphenol A from aqueous solution onto activated carbons with different modification treatments, *J. Hazard. Mater.* 164 (2009) 1275–1280.
- [11] W.-T. Tsai, C.-W. Lai, T.-Y. Su, Adsorption of bisphenol-A from aqueous solution onto minerals and carbon adsorbents, *J. Hazard. Mater.* 134 (2006) 169–175.
- [12] B. Pan, D. Lin, H. Mashayekhi, B. Xing, Adsorption and hysteresis of bisphenol A and 17 $\alpha$ -ethinyl estradiol on carbon nanomaterials, *Environ. Sci. Technol.* 42 (2008) 5480–5485.
- [13] L. Joseph, Q. Zaib, I.A. Khan, N.D. Berge, Y.-G. Park, N.B. Saleh, Y. Yoon, Removal of bisphenol A and 17 $\alpha$ -ethinyl estradiol from landfill leachate using single-walled carbon nanotubes, *Water Res.* 45 (2011) 4056–4068.
- [14] M. Clara, B. Strenn, E. Saracevic, N. Kreuzinger, Adsorption of bisphenol-A, 17 $\beta$ -estradiol and 17 $\alpha$ -ethinylestradiol to sewage sludge, *Chemosphere* 56 (2004) 843–851.
- [15] Y. Zhou, P. Lu, J. Lu, Application of natural biosorbent and modified peat for bisphenol A removal from aqueous solutions, *Carbohydr. Polym.* 88 (2012) 502–508.
- [16] J. Li, B. Zhou, Y. Liu, Q. Yang, W. Cai, Influence of the coexisting contaminants on bisphenol A sorption and desorption in soil, *J. Hazard. Mater.* 151 (2008) 389–393.
- [17] Q. Sui, J. Huang, Y. Liu, X. Chang, G. Ji, S. Deng, T. Xie, G. Yu, Rapid removal of bisphenol A on highly ordered mesoporous carbon, *J. Environ. Sci.* 23 (2011) 177–182.
- [18] J. Lee, O.K. Farha, J. Roberts, K.A. Scheidt, S.T. Nguyen, J.T. Hupp, Metal-organic framework materials as catalysts, *Chem. Soc. Rev.* 38 (2009) 1450–1459.
- [19] F.-X. Qin, S.-Y. Jia, Y. Liu, X. Han, H.-T. Ren, W.-W. Zhang, J.-W. Hou, S.-H. Wu, Metal-organic framework as a template for synthesis of magnetic CoFe<sub>2</sub>O<sub>4</sub> nanocomposites for phenol degradation, *Mater. Lett.* 101 (2013) 93–95.
- [20] J.R. Li, J. Sculley, H.C. Zhou, Metal-organic frameworks for separations, *Chem. Rev.* 112 (2011) 869–932.
- [21] I. Erucar, S. Keskin, Screening metal-organic framework-based mixed-matrix membranes for CO<sub>2</sub>/CH<sub>4</sub> separations, *Ind. Eng. Chem. Res.* 50 (2011) 12606–12616.
- [22] P. Horcajada, T. Chalati, C. Serre, B. Gillet, C. Sebrie, T. Baati, J.F. Eubank, D. Heurtaux, P. Clayette, C. Kreuz, J.-S. Chang, Y.K. Hwang, V. Marsaud, P.-N. Bories, L. Cynober, S. Gil, G. Férey, P. Couvreur, R. Gref, Porous metal-organic-framework nanoscale carriers as a potential platform for drug delivery and imaging, *Nat. Mater.* 9 (2010) 172–178.
- [23] P. Horcajada, C. Serre, M. Vallet-Regi, M. Sebban, F. Taulelle, G. Férey, Metal-organic frameworks as efficient materials for drug delivery, *Angew. Chem. Int. Ed.* 45 (2006) 5974–5978.
- [24] D. Zhao, S. Tan, D. Yuan, W. Lu, Y.H. Rezenom, H. Jiang, L.-Q. Wang, H.-C. Zhou, Surface functionalization of porous coordination nanocages via click chemistry and their application in drug delivery, *Adv. Mater.* 23 (2011) 90–93.
- [25] D. Frahm, M. Fischer, F. Hoffmann, M. Froba, An interpenetrated metal-organic framework and its gas storage behavior: Simulation and experiment, *Inorg. Chem.* 50 (2011) 11055–11063.
- [26] L.J. Murray, M. Dinca, J.R. Long, Hydrogen storage in metal-organic frameworks, *Chem. Soc. Rev.* 38 (2009) 1294–1314.
- [27] H.-L. Jiang, Y. Tatsu, Z.-H. Lu, Q. Xu, Non-, micro-, and mesoporous metal-organic framework isomers: Reversible transformation, fluorescence sensing, and large molecule separation, *J. Am. Chem. Soc.* 132 (2010) 5586–5587.
- [28] F.-X. Qin, S.-Y. Jia, F.-F. Wang, S.-H. Wu, J. Song, Y. Liu, Hemin@metal-organic framework with peroxidase-like activity and its application to glucose detection, *Catal. Sci. Technol.* 3 (2013) 2761–2768.
- [29] K.A. Cychoz, A.G. Wong-Foy, A.J. Matzger, Liquid phase adsorption by microporous coordination polymers: Removal of organosulfur compounds, *J. Am. Chem. Soc.* 130 (2008) 6938–6939.
- [30] N.A. Khan, S.H. Jung, Remarkable adsorption capacity of CuCl<sub>2</sub>-loaded porous vanadium benzenedicarboxylate for benzothiophene, *Angew. Chem. Int. Ed.* 124 (2012) 1224–1227.
- [31] E. Haque, J.E. Lee, I.T. Jang, Y.K. Hwang, J.-S. Chang, J. Jegal, S.H. Jung, Adsorptive removal of methyl orange from aqueous solution with metal-organic frameworks, porous chromium-benzenedicarboxylates, *J. Hazard. Mater.* 181 (2010) 535–542.
- [32] C. Chen, M. Zhang, Q. Guan, W. Li, Kinetic and thermodynamic studies on the adsorption of xylenol orange onto MIL-101(Cr), *Chem. Eng. J.* 183 (2012) 60–67.
- [33] S.-H. Huo, X.-P. Yan, Metal-organic framework MIL-100(Fe) for the adsorption of malachite green from aqueous solution, *J. Mater. Chem.* 22 (2012) 7449–7455.
- [34] M. Maes, M. Trekels, M. Boulhout, S. Schouteden, F. Vermoortele, L. Alaerts, D. Heurtaux, Y.-K. Seo, Y.K. Hwang, J.-S. Chang, I. Beurroies, R. Denoyel, K. Temst, A. Vantomme, P. Horcajada, C. Serre, D.E. De Vos, Selective removal of n-heterocyclic aromatic contaminants from fuels by lewis acidic metal-organic frameworks, *Angew. Chem. Int. Ed.* 123 (2011) 4296–4300.
- [35] S.H. Jung, J.H. Lee, J.W. Yoon, C. Serre, G. Férey, J.S. Chang, Microwave synthesis of chromium terephthalate MIL-101 and its benzene sorption ability, *Adv. Mater.* 19 (2007) 121–124.
- [36] F. Ke, L.-G. Qiu, Y.-P. Yuan, F.-M. Peng, X. Jiang, A.-J. Xie, Y.-H. Shen, J.-F. Zhu, Thiol-functionalization of metal-organic framework by a facile coordination-based postsynthetic strategy and enhanced removal of Hg<sup>2+</sup> from water, *J. Hazard. Mater.* 196 (2011) 36–43.
- [37] M. Maes, S. Schouteden, L. Alaerts, D. Depla, D.E. De Vos, Extracting organic contaminants from water using the metal-organic framework CrIII(OH)<sub>2</sub>{O<sub>2</sub>C-C<sub>6</sub>H<sub>4</sub>-CO<sub>2</sub>}, *Phys. Chem. Chem. Phys.* 13 (2011) 5587–5589.
- [38] Z. Hasan, J. Jeon, S.H. Jung, Adsorptive removal of naproxen and clofibrac acid from water using metal-organic frameworks, *J. Hazard. Mater.* 209–210 (2012) 151–157.
- [39] C.-X. Yang, X.-P. Yan, Selective adsorption and extraction of C70 and higher fullerenes on a reusable metal-organic framework MIL-101(Cr), *J. Mater. Chem.* 22 (2012) 17833–17841.

- [40] N.A. Khan, Z. Hasan, S.H. Jhung, Adsorptive removal of hazardous materials using metal-organic frameworks (MOFs): A review, *J. Hazard. Mater.* 244–245 (2013) 444–456.
- [41] A.A. Adeyemo, I.O. Adeoye, O.S. Bello, Metal organic frameworks as adsorbents for dye adsorption: Overview, prospects and future challenges, *Toxicol. Environ. Chem.* 94 (2012) 1846–1863.
- [42] G. Férey, C. Mellot-Draznieks, C. Serre, F. Millange, J. Dutour, S. Surble, I. Margiolaki, A chromium terephthalate-based solid with unusually large pore volumes and surface area, *Science* 309 (2005) 2040–2042.
- [43] P. Horcajada, S. Surble, C. Serre, D.-Y. Hong, Y.-K. Seo, J.-S. Chang, J.-M. Greneche, I. Margiolaki, G. Férey, Synthesis and catalytic properties of MIL-100(Fe), an iron(III) carboxylate with large pores, *Chem. Commun.* (2007) 2820–2822.
- [44] D.-Y. Hong, Y.K. Hwang, C. Serre, G. Férey, J.-S. Chang, Porous chromium terephthalate MIL-101 with coordinatively unsaturated sites: Surface functionalization, encapsulation, sorption and catalysis, *Adv. Funct. Mater.* 19 (2009) 1537–1552.
- [45] S.-H. Huo, X.-P. Yan, Metal-organic framework MIL-100(Fe) for the adsorption of malachite green from aqueous solution, *J. Mater. Chem.* 22 (2012) 7449–7455.
- [46] E.Y. Park, Z. Hasan, N.A. Khan, S.H. Jhung, Adsorptive removal of bisphenol-a from water with a metal-organic framework, a porous chromium-benzenedicarboxylate, *J. Nanosci. Nanotechnol.* 13 (2013) 2789–2794(2786).
- [47] M. Zhou, Y.-N. Wu, J. Qiao, J. Zhang, A. McDonald, G. Li, F. Li, The removal of bisphenol A from aqueous solutions by MIL-53(Al) and mesostructured MIL-53(Al), *J. Colloid Interface Sci.* 405 (2013) 157–163.
- [48] O.I. Lebedev, F. Millange, C. Serre, G. Van Tendeloo, G. Férey, First direct imaging of giant pores of the metal-organic framework MIL-101, *Chem. Mater.* 17 (2005) 6525–6527.
- [49] P. Horcajada, S. Surble, C. Serre, D.Y. Hong, Y.K. Seo, J.S. Chang, J.M. Greneche, I. Margiolaki, G. Férey, Synthesis and catalytic properties of MIL-101(Fe), an iron(III) carboxylate with large pores, *Chem. Commun.* (2007) 2820–2822.
- [50] Y.S. Ho, G. McKay, Pseudo-second order model for sorption processes, *Process Biochem.* 34 (1999) 451–465.
- [51] B.H. Hameed, A.A. Rahman, Removal of phenol from aqueous solutions by adsorption onto activated carbon prepared from biomass material, *J. Hazard. Mater.* 160 (2008) 576–581.
- [52] Z. Hasan, J. Jeon, S.H. Jhung, Adsorptive removal of naproxen and clofibric acid from water using metal-organic frameworks, *J. Hazard. Mater.* 209–210 (2012) 151–157.
- [53] E. Haque, J.W. Jun, S.H. Jhung, Adsorptive removal of methyl orange and methylene blue from aqueous solution with a metal-organic framework material, iron terephthalate (MOF-235), *J. Hazard. Mater.* 185 (2011) 507–511.
- [54] I.A.W. Tan, A.L. Ahmad, B.H. Hameed, Adsorption isotherms, kinetics, thermodynamics and desorption studies of 2,4,6-trichlorophenol on oil palm empty fruit bunch-based activated carbon, *J. Hazard. Mater.* 164 (2009) 473–482.
- [55] G. Xiao, L. Fu, A. Li, Enhanced adsorption of bisphenol a from water by acetylaniline modified hyper-cross-linked polymeric adsorbent: Effect of the cross-linked bridge, *Chem. Eng. J.* 191 (2012) 171–176.
- [56] A.T. Mohd Din, B.H. Hameed, A.L. Ahmad, Batch adsorption of phenol onto physiochemical-activated coconut shell, *J. Hazard. Mater.* 161 (2009) 1522–1529.
- [57] V. Fierro, V. Torné-Fernández, D. Montané, A. Celzard, Adsorption of phenol onto activated carbons having different textural and surface properties, *Microporous Mesoporous Mater.* 111 (2008) 276–284.
- [58] Y. Yoon, P. Westerhoff, S.A. Snyder, M. Esparza, Hplc-fluorescence detection and adsorption of bisphenol a, 17 $\beta$ -estradiol, and 17 $\alpha$ -ethynyl estradiol on powdered activated carbon, *Water Res.* 37 (2003) 3530–3537.
- [59] Y. Dong, D. Wu, X. Chen, Y. Lin, Adsorption of bisphenol A from water by surfactant-modified zeolite, *J. Colloid Interface Sci.* 348 (2010) 585–590.
- [60] G. Newcombe, M. Drikas, Adsorption of nom onto activated carbon: Electrostatic and non-electrostatic effects, *Carbon* 35 (1997) 1239–1250.